Journal Name

ARTICLE TYPE

Microwave-assisted synthesis of Bi$_2$Se$_3$ ultrathin nanosheets and its electrical conductivities†

Haiming Xu,[a] Gang Chen,*[a] Rencheng Jin,[b] Dahong Chen,[a] Yu Wang,[a] Jian Pei,[a] Yongqiang Zhang,[a] Chunshuang Yan[a] and Zhuangzhuang Qiu[a]

Ultrathin Bi$_2$Se$_3$ nanosheets have been successfully fabricated through microwave-assisted approach in the presence of ethylene glycol (EG) under 1 kW microwave power for 1 minute. The structure and morphology of the obtained products were characterized by powder X-ray diffraction (XRD), field-
10 emission scanning electron microscopy (FESEM), transmission electron microscopy (TEM), high-resolution TEM (HRTEM), selected-area electron diffraction (SAED) and Raman spectroscopy techniques. Based on the control experimental, a possible growth mechanism of Bi$_2$Se$_3$ ultrathin nanosheets was proposed. Furthermore, the thermoelectric transport properties of the nanosheets are investigated by measuring the electrical conductivity and the Seebeck coefficient at temperature ranging
15 from 298 to 523 K. The maximum power factor can reach 157 μW m^{-1} K^{-2} at 523 K due to the ultrathin nature of the as-prepared sample, indicating the promising approach can extend to synthesize other thermoelectrical materials.

Introduction

Bismuth selenide, a V-VI semiconductor with a band gap of
20 ~0.3eV,[1–3] belongs to a class of narrow band gap layered semiconductors with tetradymite structure having space group R$\bar{3}$m–D$^5_{3d}$. Due to the existence of six valley degeneracy and the narrow energy gap, Bi$_2$Se$_3$ has attracted much attention for their potential applications in thermoelectric, electrochemical
25 hydrogen storage, optoelectronic devices, photoelectrochemical cells and IR spectroscopy etc.[4–14] For applications in these aspects, many methods have been proposed for the synthesis of Bi$_2$Se$_3$, including the single-source precursor method,[15] solvothermal method,[16, 17] metalorganic chemical vapor
30 deposition method,[18] Bridgman technique,[19] and so on. However, these approaches generally require harsh experimental conditions, high energy consumption, long reaction time and toxic reducing agents or solvent, which pose potential environmental and ecology risks. In order to overcome these shortcomings, a simple,
35 rapid, low cost and environment-friendly approach for the preparation of Bi$_2$Se$_3$ is expected.

Microwave heating in the synthesis of nanomaterials has attracted much attention during the past decades.[20–22] Compared with microwave heating, conventional heating is rather slow and
40 inefficient for transferring energy to reaction mixture. Furthermore, traditional heating depends on convective currents and thermal conductivity of different materials, and usually cause the reaction vessel temperature higher than that of reaction solution. On the contrary, microwave (MW) irradiation realizes
45 the efficient internal volumetric heating by direct transmission of MW energy into the molecules present in the reaction mixture.[23] Therefore the temperature uniformly raised throughout the whole liquid volume while without thermal gradients,[24] favor well-defined morphology products synthesized[25] and save a lot of
50 energy.[26] Besides, rapid heating could dramatically save reaction time by orders of magnitude, elevate rate constant[27] and increase product yield.[28] Due to these merits, microwave methodology has been widely used as a promising technique in the synthesis of nanostructure materials. For instance, Bilecka et al. prepared ZnO
55 nanoparticles from zinc acetate and benzyl alcohol with microwave irradiation.[24] Sb$_2$Te$_3$ nanosheets having edge lengths of 300–500 nm and thicknesses of 50–70 nm were rapidly synthesized with microwave-assisted method by Zhu's group.[29] R. Harpeness et al. fabricated leaf-like Bi$_2$Se$_3$ by the microwave-
60 assisted synthesis in the ethylene glycol solution.[30] However, these synthesize process present long reaction time (20–40 minutes) which means consumption more energy. Therefore, in order to saving energy and enhance efficiency, fast (1 minute or less) and simple method is necessary.

65 In this work, we report a "green" and fast approach for the fabrication of ultrathin Bi$_2$Se$_3$ nanosheets in the presence of EG at a reaction temperature of 180 °C for 1 min. Furthermore, the thermoelectric transport properties of the ultrathin Bi$_2$Se$_3$ nanosheets has been investigated and shown good performances,
70 which suggesting that this promising method can expand to the fabrication of other material.

Experimental

Materials and synthesis procedures

All chemicals were analytical grade and used without further
75 purification. In a typical synthesis, a stoichiometric ratio of

bismuth nitrate (Bi(NO$_3$)$_3$•5H$_2$O, 0.2424 g), sodium selenide (Na$_2$SeO$_3$, 0.1297 g) and potassium hydroxide (KOH, 0.5 g) were dissolved in 50 ml ethylene glycol in 100 mL flasks at room temperature. After vigorous stirring for 5 min, the mixture was
5 microwave-heated to 180 ºC for 1 minute with power 1000 W. When cooling to room temperature, the product was separated by centrifugation, washed with deionized water and absolute ethanol several times, and then dried at 60 ºC in a vacuum for 8h. The microwave oven used was a focused multi-mode microwave
10 synthesis system (2.45 GHz, maximum 1000 W, MAS-II, Sineo, China), which was equipped with magnetic stirring and a water-cooled condenser. Temperature was controlled by automatic adjustment of the microwave power.

Characterization

15 XRD patterns were recorded over the 2θ range from 10º to 90º at a speed of 10º min^{-1} using a Rigaku D/max-2000 device equipped with Cu Kα radiation (λ = 0.15406 nm). Field-emission scanning electron microscopy (FESEM, FEI, Quanta 200F) and transmission electron microscopy (TEM, FEI, Tecnai G2 S-Twin)
20 were employed to observe the morphology of the samples. Raman spectroscopy was recorded (Horiba Jobin Yvon CO. Ltd) using a 632.8 nm laser with an incident power of 0.5 mW.

Thermoelectric transport measurement

To measure the electrical conductivity and Seebeck coefficient of
25 the as-prepared samples, the bar-shaped samples (10 × 4.52 × 0.45 mm^3) were prepared under 20 MPa pressure at room temperature. Then, the sample was sintered for 6 seconds in a microwave oven (G80F23CSL-X2(G0), Galanz, China) under vacuum conditions. Silver paste electrodes coated on the
30 specimen were used as electrical contacts. The four-probe technique was employed for the electrical conductivity measurement. For the measurement of the Seebeck coefficient, a micro-heater was applied to create a temperature difference (about 3–15 K) between the cool and hot ends of the specimen. A
35 temperature gradient was established in the samples when the electrical power was applied by a thermoelectric pile. Two thermocouples were contacted to the surface of the sample to detect the temperature drop (DT), while the resulting thermally induced voltage DV was tested by the voltage probes. Then the
40 Seebeck coefficient can be obtained by the formula, $S = -\Delta V/\Delta T$. The data of electrical conductivity and Seebeck coefficient were collected by a computer-controlled multifunctional measuring system with a flow of argon 1 mL min^{-1} (Keithley 2400 source meter, Keithley 2700 multimeter, Keithley Instruments Inc.,
45 USA).

Results and discussion

Characterization of ultrathin Bi$_2$Se$_3$ nanosheets

The phase purity and crystal structure of the as-prepared sample has been identified by X-ray diffraction and the pattern is shown
50 in Fig. 1a. In this pattern, all the diffraction peaks can be steadily indexed to the rhombohedra crystal geometry of Bi$_2$Se$_3$ (JCPDS: 33–0214). No characteristic peaks for impurities are observed, suggesting the high purity of the final product. Moreover, the sharp peaks suggest that the as-prepared Bi$_2$Se$_3$ nanosheets are
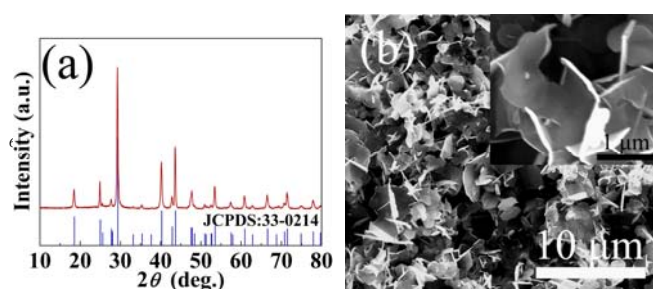55 highly crystalline under the present procedure. Fig. 1b is a typical

Fig. 1 XRD patterns (a) and FESEM image of the as-prepared sample with microwave-assisted heating in EG solution at 180 ºC for 1 minute.

low scanning electron microscopy (SEM) image of the Bi$_2$Se$_3$ product, revealing that the product consists of uniform nanosheets
70 with an average diameter of 1–2 μm (Fig.S1 ESI†). The magnified image in Fig. 1b (upper corner) shows that the nanosheets have hexagonal like structures. Further observed, the thickness of nanosheets, which are intercrossed with each other, is in the range of 30–40 nm (Fig.S1 ESI†).
75 In order to further investigate the microstructure of the nanosheets, transmission electron microscopy (TEM), high resolution transmission electron microscopy (HRTEM) and selected area electron diffraction (SAED) measurements were carried out. The TEM images (Fig. 2a and b) clearly reveal that
80 the as-prepared sample is a well-defined nanosheets, which agreed well with the SEM observation. The HRTEM image of the Bi$_2$Se$_3$ is shown in Fig. 2c. The lattice fringe clearly revealed the presence of the (015) plane with a lattice spacing of 0.304 nm. The corresponding selected area electron diffraction (SAED)
85 pattern of the ultrathin Bi$_2$Se$_3$ nanosheets are presented in Fig. 2d and the electron diffraction pots indicate the single crystalline nature of Bi$_2$Se$_3$ nanosheets.

The Raman spectrum of the ultrathin Bi$_2$Se$_3$ nanosheets (wavenumber range 80–600 cm^{-1}) at room temperature is shown
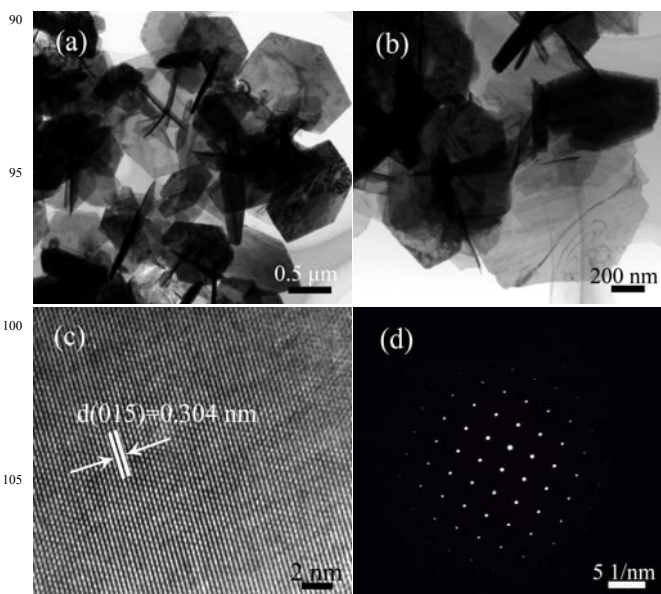

Fig. 2 The structure and morphology of the ultrathin Bi$_2$Se$_3$ nanosheets: (a)
110 low magnification SEM image, (b) high magnification SEM image, (c) HRTEM image recorded for an individual nanosheet, (d) SAED pattern of the nanosheets.
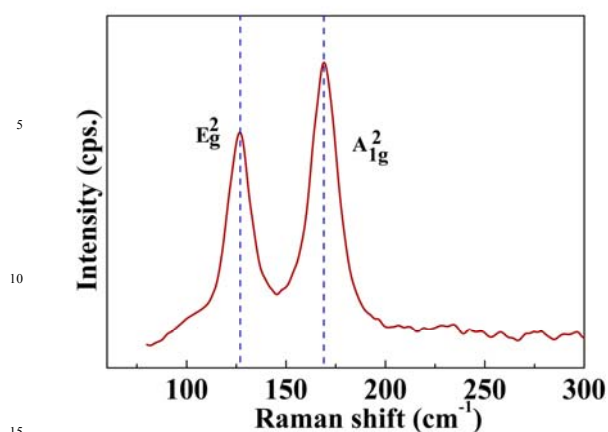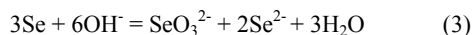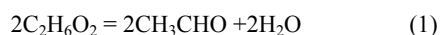
Fig. 3 Raman spectrum of the ultrathin Bi_2Se_3 nanosheets, Raman spectrum on the nanosheets was recorded in the range of 80–600 cm^{-1}; however, for clarity, Raman shifts are shown for 80–300 cm^{-1}.

in Fig. 3. There are two distinct peaks of the as-prepared sample at 130 cm^{-1} and 171 cm^{-1} within the scanned frequency range. No significantly red or blue shift can be observed. According to the Raman selection rules given in the previous reports,[31, 32] it follows that the peak at 130 cm^{-1} is attributed to the E_g^2 mode, and another peak (171 cm^{-1}) corresponds to A_{1g}^2 mode, which are agree well with the previously experimental results and calculated phonon vibration modes of pure Bi_2Se_3.[2, 33] Furthermore, no other impurity peaks appear in the Raman spectrum. Therefore, according to the above XRD, TEM, SAED results and Raman analysis, the well-defined hexagonal Bi_2Se_3 ultrathin nanosheets can be successfully synthesized at 180 ºC with 1 minute.

Formation Mechanism of ultrathin Bi_2Se_3 nanosheets

A possible schematic diagram of the as-prepared sample is depicted in Fig. 4. According to Zhang et al., Wang et al. and Sun et al., the ethylene glycol (EG) can oxidation to acetaldehyde under a high temperature and used as reducing agent (equation (1)). In the initial stage, Na_2SeO_3 will firstly dissociate itself and form SeO_3^{2-} in reaction solution, and then the SeO_3^{2-} ions were rapidly reduced by ethylene glycol (EG) to form elemental Se upon microwave heating(equation (2)).[34–36] The fresh generated selenium (even Se_n molecule dissolved in solution before their aggregation) has high reaction activity, and it is prone to produce Se^{2-} through disproportionation under alkaline conditions (equation (3)).[37, 38] Then the Se^{2-} ions reacted with Bi^{3+} ions to form Bi_2Se_3 (equation 4). Consequently, the chemical reactions to form Bi_2Se_3 can be expressed as follows:

$$2C_2H_6O_2 = 2CH_3CHO + 2H_2O \qquad (1)$$

$$2CH_3CHO + SeO_3^{2-} = 2CH_3COO^- + Se + H_2O \qquad (2)$$

$$3Se + 6OH^- = SeO_3^{2-} + 2Se^{2-} + 3H_2O \qquad (3)$$

$$3Se^{2-} + 2Bi^{3+} = Bi_2Se_3 \qquad (4)$$

To investigate that the formation mechanism of bismuth selenide is atomic or ionic mechanism, we designed a series control experimentals while keep other conditions unchanged.
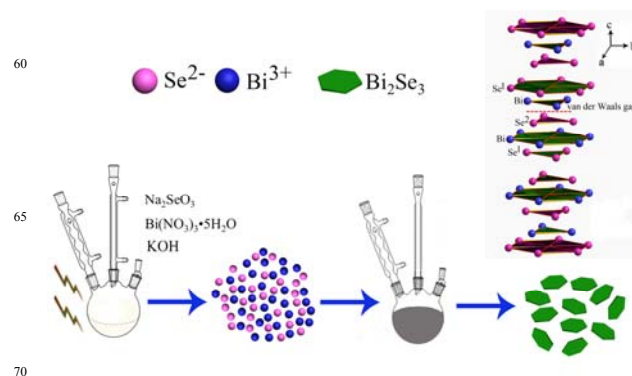

Fig. 4 Schematic illustration of the proposed formation mechanism of the Bi_2Se_3 nanosheets. The right corner image is the crystal structure of Bi_2Se_3.

When the reaction finished with no KOH, there was no product obtained while the mixture transformed from transparent to brick red which attribute to amorphous selenium produced.[4] This phenomenon reveals that in the absence of potassium hydroxide, although SeO_3^{2-} could be reduced by ethylene glycol,[35] the fresh selenium did not disproportion to selenium ions.[38] Moreover, when keep other conditions unchanged while with free Na_2SeO_3, the mixture remained transparent(no products) after the reaction completed, suggesting that no Bi_2O_3 or Bi $(OH)_3$ produced under the present conditions.[4] Therefore, according to the above analysis, we proposed that the ionic mechanism is the main mechanism of Bi_2Se_3 synthesis in the present system.

Why the synthetic bismuth selenide is hexagonal nanoplatelets? As well known, Bi_2Se_3 crystallizes in a different crystal structure with a hexagonal unit cell (Fig. 4, right corner), where a Bi layer is made up of Bi atoms arranged to form a plane hexagonal structure, and a Se layer formed by Se atoms arranged in the same way, non-compact hexagonal layers perpendicular to the c-axis.[39] As shown in Fig. 4, a unit cell is packed with two Bi layers and three Se layers following the pattern: $[Se^1-Bi-Se^2-Bi-Se^1]$.[9, 32] The Se^1 atoms occupy the boundary layers of the unit cell. The bonds within these layers are generally considered to be predominantly covalent, and those between them are due to van der Waals forces. This structural arrangement leads to an easy cleavage of the (0001) planes, and crystal growth occurs in the [1010] directions, which contributes to the formation of hexagon flake-like Bi_2Se_3 crystals.[40, 41] Besides, microwave (MW) heating has the so-called "specific" or "non-thermal" MW effects caused dramatically boost the reduction reaction rate,[23] thereby resulting in fast nucleation and growth. As a result, small Bi_2Se_3 nanoparticles were obtained. Meanwhile, the formed sheet bismuth selenide difficult grow up by Ostwald ripening owing to the reaction time is very short. As a result, ultrathin Bi_2Se_3 nanosheets with narrow size distribution were obtained.

Electrical transportation properties

To measure the electrical transport properties of the obtained ultrathin Bi_2Se_3 nanosheets, the samples were first pressed into a monolith with a rectangular shape of about $10 \times 4.6 \times 0.5$ mm^3, and then treated by microwave sintering for 6s under vacuum condition.[4, 9] Bars of ultrathin Bi_2Se_3 nanosheets finally appear with a density of 5.73 g cm^{-3} (84% of theoretical density). Fig. 5a
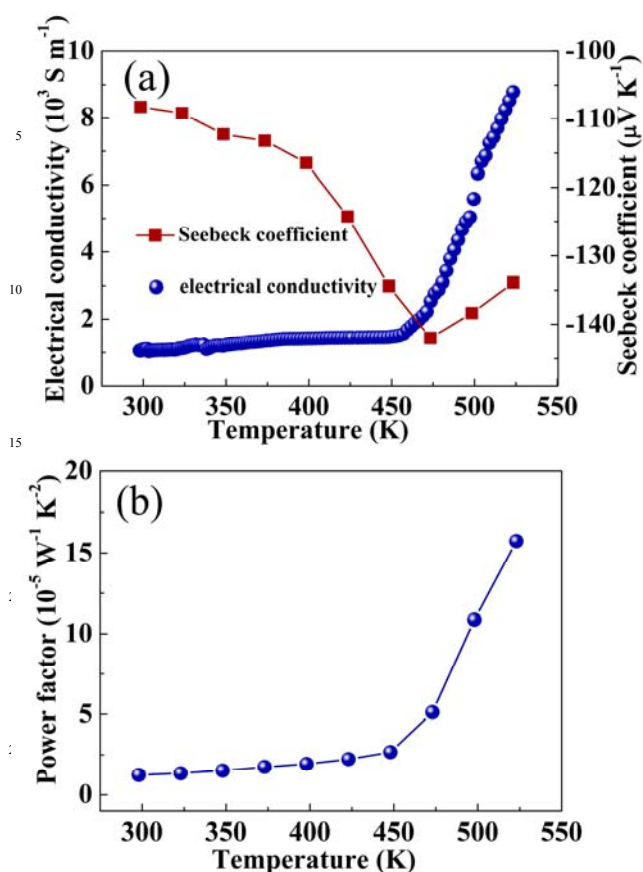
Fig. 5 Temperature dependence of thermoelectric properties of the prepared samples: (a) electrical conductivity and Seebeck coefficient, (c) power factor.

shows the plot of the electrical conductivities (σ) versus the temperature measured in the range of 300–523 K using the four probes technique. The electrical conductivity (σ) increases linearly with temperature from 1.06×10^3 S m^{-1} at 300 K to 8.8×10^3 S m^{-1} at 523 K, with typical semiconducting behaviour for the entire measuring temperature range. The electrical conductivity of the as-prepared sample is larger than our group`s former reported (7.12×10^3 S m^{-1} at 523 K, the Bi$_2$Se$_3$ nanosheets synthesized at 180 ºC for 25 min with the thickness range from 50 nm to 100 nm).[9] The reasonably high σ value is by virtue of the ultra-thin nature of the nanosheets in which the dominant surface states can offer high mobility, scattering-resistant carriers to enhanceσ.[42] The greater electronic density of states at the conduction band of ultrathin Bi$_2$Se$_3$ nanosheets can further increaseσ.[43, 44] Therefore, obtain an excellent electrical conductivity of the sample.

Fig. 5a shows the plot of the Seebeck coefficient (S) versus the temperature measured in the range of 300–523 K. The graph shows that absolute Seebeck coefficient increases with temperature, attains a maximum value (144 µV K^{-1}) around 498 K, and then decreases. The negative Seebeck coefficient of the as-prepared sample reveals that the as-prepared ultrathin Bi$_2$Se$_3$ nanosheets are n-type semiconductor result from a high density of selenium vacancies,[45] which is expected for Bi$_2$Se$_3$. Kadel et al. have also reported a similar result for the Seebeck coefficient for n-type Bi$_2$Se$_3$ that shows the maximum Seebeck coefficient value at about 400 K.[46] This phenomenon attribute to the fact that the as-prepared sample is typical semiconductor, as the temperature increases, the excitation of the carriers from the valence band to the conduction band becomes easier, thus more carriers will be involved in conductivity, resulting in an increase in the electrical conductivity reverse reduce the Seebeck coefficient of the samples.[4, 47, 48]

The corresponding power factor of the sample displayed in Fig. 5b shows the dependence of the power factor on increases with the temperature. The increase in power factor with the temperature can attributed to the increase in the electrical conductivity with temperature due to the semiconducting nature of the sample itself. The maximum value of the power factor is 15.7×10^{-5} W m^{-1} K^{-2} at 523 K, and the room temperature value is 1.2×10^{-5} W m^{-1} K^{-2}, which can compared to the power factor of Bi$_2$Se$_3$ nanoplates (15×10^{-5} W m^{-1} K^{-2}, 523 K).[46] Moreover, it is noteworthy that nanostructuring could provide an efficient strategy to decrease thermal conductivity through the enhanced phonon scattering at the numerous grain boundaries and interfaces.[42, 49] In this work, the ultrathin Bi$_2$Se$_3$ nanosheets endow the sample with very high interface and boundary densities, which can effectively scatter mid/long-wavelength phonons and hence contribute to reducing thermal conductivity.[50, 51]Thus, a considerable ZT value can be expected in this ultrathin Bi$_2$Se$_3$ material.

Conclusions

In summary, ultrathin Bi$_2$Se$_3$ nanosheets have been successfully synthesized by a "green" and facile method in the presence of EG at a reaction temperature of 180 °C for 1 minute. The power factor of the sample can reach up to 15.7×10^{-5} W m^{-1} K^{-2} at 523 K, which higher than the literature report. Moreover, this work confirms that ultrathin nature nanosheets can significantly enhance the electrical conductivity of the sample due to large surface states, which may be a promising approach for the development of new types of highly efficient thermoelectric materials.

Acknowledgement

References

Department of Chemistry, Harbin Institute of Technology, Harbin 150001, P. R. China. E-mail: gchen@hit.edu.cn; Fax: (+86)-451-86413753; Tel: (+86)-0451-86413753
†Electronic Supplementary Information (ESI) available: [The diameter and thickness size distribution of the as-prepared samples]

1 L. E. Bell, *Science*, 2008, **321**, 1457-1461.
2 E. Y. Wang, H. Ding, A. V. Fedorov, W. Yao, Z. Li, Y. F. Lv, K. Zhao, L.G. Zhang, Z. J. Xu, J. Schneeloch, R. D. Zhong, S. H. Ji, L. L. Wang, K. He, X. C. Ma, G. D. Gu, H. Yao, Q. K. Xue, X. Chen and S. Y. Zhou, *Nature Physics*, 2013, **9**, 621–625.
3 C. Mann, D. West, I. Miotkowski, Y. P. Chen, S. B. Zhang and C. K. Shih, *Nature Communications* 2013, **4**, 2277.
4 H. M. Xu, G. Chen, R. C. Jin, D. H. Chen, J. Pei and Y. Wang, *CrystEngComm*, 2013, **15**, 5626–5632.

5 B. Zhang, X. Ye, W. Hou, Y. Zhao and Y. Xie, *J. Phys. Chem. B,* 2006, **110**, 8978–8985.

6 J. Waters, D. Crouch, J. Raftery and P. O'Brien, *Chem. Mater.,* 2004, **16**, 3289–3298.

7 L. S. Li, R. G. Cao, Z. J. Wang, J. J. Li and L. M. Qi, *J. Phys. Chem. C,* 2009, **113**, 18075–18081.

8 Z. L. Sun, S. C. Liu, X. H. Chen and L. D. Chen, *Chem. Commun.,* 2010, **46**, 3101–3103.

9 H. M. Xu, G. Chen, R. C. Jin, J. Pei, Y. Wang and D. H. Chen, *CrystEngComm,* 2013, **15**, 1618–1625.

10 J. Li, Y. C. Zhu, J. Du, J. H. Zhang and Y. T. Qian, *Solid State Commun.,* 2008, **147**, 36–40.

11 Y. F. Lin, H. W. Chang, S. Y. Lu and C. W. Liu, *J. Phys. Chem. C,* 2007, **111**, 18538–18544.

12 C. Yang, H. B. Zhao, Y. L. Hou and D. Ma, *J. Am. Chem. Soc.,* 2012, **134**, 15814–15821.

13 J. J. Wu, J. H. Zhu, M. G. Zhou, Y. L. Hou and S. Gao, *CrystEngComm,* 2012, **14**, 7572–575.

14 H. B. Liao and Y. L. Hou, *Chem. Mater.,* 2013, **25**, 457–465.

15 S. T. Manjare, S. Yadav, H. B. Singh and R. J. Butcher, *Eur. J. Inorg. Chem.,* 2013, **30**, 5344–5357.

16 D. S. Kong, K. J. Koski, J. J. Cha, S. S. Hong and Y. Cui, *Nano Lett.,* 2013, **13**, 632–636.

17 R. C. Jin, J. S. Liu, Y. B. Xu, G. H. Li, G. Chen and L. X. Yang, *J. Mater. Chem. A,* 2013, **1**, 10942–10950.

18 L. D. Alegria, M. D. Schroer, A. Chatterjee, G. R. Poirier, M. Pretko, S. K. Patel and J. R. Petta, *Nano Lett.,* 2012, **12**, 4711–4714.

19 J. Kasparova, C. Drasar, A. Krejcova, L. Benes, P. Lostak, W. Chen, Z. H. Zhou and C. Uher, *J. Appl. Phys.,* 2005, **97**, 103720.

20 D. Borah, R. Senthamaraikannan, S. Rasappa, B. Kosmala, J. D Holmes and M. A Morris, *ACS Nano,* 2013, **7**, 6583–6596.

21 Y. R. Wang, W. L. Yang, L. Zhang, Y. Hu and X. W. Lou, *Nanoscale,* 2013, **5**, 10864–10867.

22 C. J. Jafta, M. K. Mathe, N. Manyala, W. D. Roos and K. I. Ozoemena, *ACS Appl. Mater. Interfaces,* 2013, **5**, 7592–7598.

23 M. Baghbanzadeh, L. Carbone, P. D. Cozzoli and C. O. Kappe, *Angew. Chem. Int. Ed.,* 2011, **50**, 11312–11359.

24 I. Bilecka, P. Elser and M. Niederberger, *ACS Nano,* 2009, **3**, 467–477.

25 Y. He, L. M. Sai, H. T. Lu, M. Hu, W. Y. Lai, Q. L. Fan, L. H. Wang and W. Huang, *Chem. Mater.,* 2007, **19**, 359–365.

26 I. Bilecka and M. Niederberger, *Nanoscale,* 2010, **2**, 1358–1374.

27 B. T. Ergan and M. Bayramoğlu, *Ind. Eng. Chem. Res.,* 2011, **50**, 6629–6637.

28 R. Hoogenboom and U. S. S. Macromol, *Rapid Commun.,* 2007, **28**, 368–386.

29 G. H. Dong, Y. J. Zhu and L. D. Chen, *J. Mater. Chem.,* 2010, **20**, 1976–1981.

30 R. Harpeness and A. Gedanken, *New J. Chem.,* 2003, **27**, 1191–1193.

31 V. Chis, I. Yu. Sklyadneva, K. A. Kokh, V. A. Volodin, O. E. Tereshchenko and E. V. Chulkov *Phys. Rev. B.,* 2012, **86**, 174304.

32 J. Zhang, Z. P. Peng, A. Soni, Y. Y. Zhao, Y. Xiong, B. Peng, J. B. Wang, M. S. Dresselhaus and Q. H. Xiong, *Nano Lett.,* 2011, **11**, 2407–2414.

33 K. M. F. Shahil, M. Z. Hossain, V. Goyal and A. A. Balandin, *J. Appl. Phys.,* 2012, **111**, 054305.

34 Y. G. Sun, Y. D. Yin, B. T. Mayers, T. Herricks and Y. N. Xia, *Chem. Mater.* 2002, **14**, 4736–4745.

35 P. Toneguzzo, G. Viau, O. Acher, F. F. Vincent and F. Fiévet, *Adv. Mater.,* 1998, **10**, 1032–1035.

36 L. H. Zhang, H. Q. Yang, J. Yu, F. H. Shao, L. Li, F. H. Zhang and H. Zhao, *J. Phys. Chem. C,* 2009, **113**, 5434–5443.

37 B. Zhou and J. J. Zhu, *Nanotechnology,* 2009, **20**, 085604.

38 D. B. Wang, D. B. Yu, M. W. Shao, J. Y. Xing and Y. T. Qian, *Mater. Chem. Phys.,* 2003, **82**, 546–550.

39 K. J. Koski, C. D. Wessells, B. W. Reed, J. J. Cha, D. S. Kong and Y. Cui, *J. Am. Chem. Soc.,* 2012, **134**, 13773–13779.

40 G. Z. Shen, D. Chen, K. B. Tang and Y. T. Qian, *Nanotechnology,* 2004, **15**, 1530–1534.

41 D. S. Kong, W. H. Dang, J. J. Cha, H. Li, S. Meister, H. L. Peng, Z. F. Liu and Y. Cui, *Nano Lett.,* 2010, **10**, 2245–2250.

42 Y. F. Sun, H. Cheng, S. Gao, Q. H. Liu, Z. H. Sun, C. Xiao, C. Z. Wu, S. Q. Wei and Y. Xie, *J. Am. Chem. Soc.,* 2012, **134**, 20294–20297.

43 M. K. Jana, K. Biswas and C. N. R. Rao, *Chem. Eur. J.,* 2013, **19**, 9110–9113.

44 Y. Sun, H. Cheng, S. Gao, Q. Liu, Z. Sun, C. Xiao, C. Wu, S. Wei and Y. Xie, *J. Am. Chem. Soc.* 2012, **134**, 20294–20297.

45 X. F. Qiu, L. N. Austin, P. A. Muscarella, J. S. Dyck and C. Burda, *Angew. Chem. Int. Ed.,* 2006, **45**, 5656–5659.

46 K. Kadel, L. Kumari, W. Z. Li, J. Y. Huang and P. P. Provencio, *Nanoscale Res. Lett.,* 2011, 6:5.

47 M. K. Han, K. Ahn, H. J. Kim, J. S. Rhyee and S. J. Kim, *J. Mater. Chem.,* 2011, **21**, 11365–11370.

48 R. C. Jin, G. Chen, J. Pei, J. X. Sun and Q. Wang, *CrystEngComm,* 2012, **14**, 4461–4466.

49 K. Takei, M. Madsen, H. Fang, R. Kapadia, S. Chuang, H. S. Kim, C. Liu, E. Plis, J. Nah, S. Krishna, Y. Chueh, J. Guo and A. Javey, *Nano Lett.,* 2012, **12**, 2060–2066

50 A. Soni, Y. Z. Yan, Y. Ligen, M. Aik, M. Dresselhaus and Q. Xiong, *Nano Lett.,* 2012, **12**, 1203–1209.

51 V. Goyal, D. Teweldebrhan and A. A. Balandin, *Appl. Phys. Lett.,* 2010, **97**, 133117.

Graphic abstract
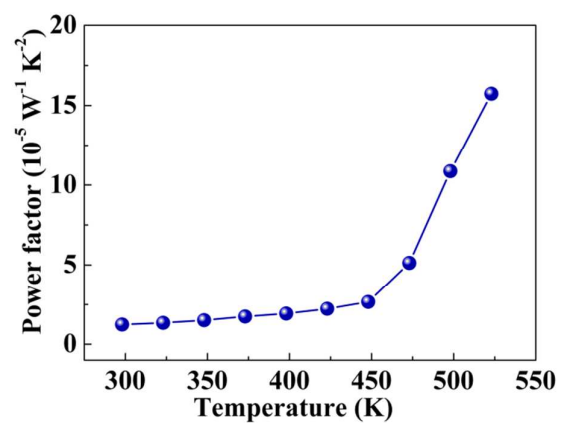
Ultrathin Bi_2Se_3 nanosheets (30 nm) have been successfully fabricated with 1 kW microwave power for 1 minute. The maximum power factor of the sample can reach to157 μW m^{-1} K^{-2} at 523 K, which larger than the sample with thickness ranging from 50 nm to 100 nm.